Evaluation of an optimal stochastic controller in a full-scale experiment

M. Nygård Ferguson and J.-L. Scartezzini
Laboratoire d'Energie Solaire et de Physique du Bâtiment, Ecole Polytechnique Fédérale de Lausanne, CH-1015 Lausanne (Switzerland)

(Received August 4, 1990; accepted December 18, 1990; revised paper received March 28, 1991)

Abstract

A predictive controller based on the theory of optimal stochastic control was developed in order to save energy and minimize overheating in buildings with significant solar gains. The random nature of solar gains and the inertia of the heating system are catered for by this controller. The predictive controller has been tested previously in passive solar rooms by computer simulations. A prototype predictive controller was developed and installed in an occupied office of a passive solar experimental building. The performance of this controller was compared to that of a conventional external temperature controller in an identical office during the heating season 1989–90. The energy consumption was 27% less for the predictive controller over the entire period. The savings varied between 0% for cloudy winter weeks to 60% for sunny spring weeks. The thermal comfort in the office with the predictive controller was improved while the savings were achieved.

Introduction

Energy consumption for heating represents a large part of the primary energy used in modern society (39% in Switzerland in 1988). One way of reducing the heating energy consumption is to construct passive solar buildings for which the solar gains may cover over 50% of the heating needs.

Solar gains are, however, of random nature and conventional, non-predictive, control algorithms can only cater for part of these gains. Overheating and thermal discomfort of the occupants are not rare during sunny days, and the excessive heat has to be extracted.

The most common reaction of the occupants is to open the windows. Air-conditioning devices can also be installed to reject the excessive heat, however they use more energy in the process.

Different deterministic controllers, investigated previously, use the prediction of stable weather fronts [1, 2], information from weather satellites [3] or predictions from weather models in combination with the theory of deterministic optimal control [4–6].

None of these controllers, however, can satisfactorily cater for the random nature of the solar gains. For this reason a predictive controller based on the theory of optimal stochastic control [7], which takes into consideration the random nature of the solar gains and the inertia of the heating system, has been developed.

The predictive controller based on the theory of optimal stochastic control has been applied to building heating control. The objective of the controller is to reduce the internal air temperatures in the mornings and overnight, in anticipation of solar gains during the day. This will result in both a reduction in energy consumption and an improvement in the thermal comfort of the occupants.

The potential for this controller has previously been demonstrated by the authors using computer simulations [8]. Detailed simulation results and parametric studies are also given in ref. 9. Similar controllers based on the same theory have been applied to solar collectors for domestic hot water by Tödtli [10], and for the application to renewable power systems with photovoltaic cells by Heinemann and Luther [11].

The predictive controller described in this paper has been implemented in a full-scale experiment using two offices with separate floor-heating systems and south-facing glazing. The principal results of the comparison between the predictive controller and a conventional external temperature controller are given here. A more detailed comparison can be found in ref. 9.

0378-7788/92/$5.00

Methods

The predictive controller used in this experiment is based on the theory of optimal stochastic control [7]. It uses different specific models and algorithms as illustrated in Fig. 1. The principal elements of this block diagram are:

(1) the cost function
(2) the stochastic model of the meteorological variables
(3) the building model
(4) calculation algorithms
(5) the matrix of optimal commands
(6) measurements (pointer in matrix)
(7) heating command (output from matrix).

The matrix of optimal commands is calculated at the beginning of each optimization period, i.e., at midnight, taking into account the meteorological conditions the previous day. An optimal command is then retrieved from the matrix each hour. The pointer into the matrix consists of the state of solar radiation, the thermal state of the building system and the hour.

The objective of the predictive controller is to minimize the cost function, which, in this case, is a function of both the thermal comfort of the occupants and the energy consumption. The way in which the cost function is defined and optimized is the distinguishing factor between different kinds of controllers.

In a conventional (non-predictive) controller the cost function is minimized at each instant of time. A deterministic predictive controller minimizes the cost function according to one prediction of the future weather evolution (certainty equivalence) for the optimization period. The calculation is often repeated when the prediction proves to be false.

The predictive controller based on optimal stochastic control, on the other hand, minimizes the *expected cost function* according to the probabilities of the future weather evolution. Conditions of existence of optimal control are not known [12]. A functional equation for the cost function can however be derived using dynamic programming [7] under the assumption that such a solution exists.

The cost function is therefore one of the key elements of the predictive controller. It defines the variables to optimize, i.e., minimize or maximize, and their respective importance over an optimization period $0 \rightarrow N$. The instantaneous cost function used in this study was:

$$J(\boldsymbol{u}, \boldsymbol{T}) = C_1 J(\boldsymbol{u}) + C_2 J_2(\boldsymbol{T})$$
$$= C_1 \boldsymbol{u} + C_2[\exp(\mathrm{PMV}^2(\boldsymbol{T})) - 1] \quad (1)$$

where $\boldsymbol{u}$ represents the energy delivered by the heating plant, $\boldsymbol{T}$ is the vector containing the temperatures of the elements of the building system, and PMV is the predicted mean vote which predicts the thermal comfort of the occupants [13].

The PMV depends on the metabolic activity of the occupants, the thermal resistance of the clothing, the wind speed, the relative humidity, the partial pressure of H_2O and the clothing factor. All these parameters have been considered constant within two time intervals which correspond to daytime activities (06:00–22:00) and nighttime activities (22:00–06:00). A PMV of 0 means that the conditions are on average optimal in terms of perceived thermal comfort; ± 1 means the conditions are acceptable (+too warm, −too cold), ± 2 the conditions are unacceptable and ± 3 the conditions are unbearable.

The weights C_1 and C_2 have been chosen such that a |PMV| increase of 0.2, e.g., at optimal comfort an increase from 5% to 6% of dissatisfied occupants, will give the same cost increase as a change from zero to maximum heating. A parametric study of C_1 and C_2 has been carried out and is presented in ref. 9. An increase of the C_2/C_1 ratio will not result in a significant increase of the thermal comfort of the occupants, while a reduction in the ratio will cause a deterioration in thermal comfort. A C_2/C_1 ratio of half the value used in the experiment would still give an acceptable thermal comfort in most situations as well as a significant reduction in energy consumption.

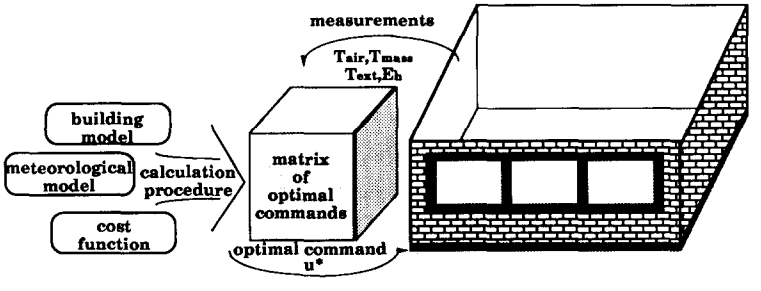

Fig. 1. Block-diagram of the predictive controller based on optimal stochastic control.

The stochastic models of the meteorological variables have previously been described in refs. 8 and 9 and are therefore not given here. Hourly weather data for the location of Lausanne, in years 1978–85, collected by the Swiss Meteorological Institute have been used to construct these models. They can be summarized as follows:

– The fraction of average daily irradiance, $r(j) = \langle E_h \rangle_j / \langle E_{h0} \rangle_j$, is the ratio between the measured $\langle E_h \rangle_j$ (W/m^2) and potential $\langle E_{h0} \rangle_j$ (W/m^2) average solar irradiance on a horizontal surface during day j. It is divided into four classes, of "type of day", and it is modelled via a Markov chain.

– The cloudiness index, $\tau = E_h / E_{h0}$, is the solar irradiance, E_h (W/m^2) divided by the maximal possible solar irradiance, E_{h0} (W/m^2). It is modelled via a Markov chain.

– One 4×4 probability matrix characterizes the daily transition (among the four classes of "type of day").

– Four 10×10 probability matrices (one for each type of day) characterize the hour-by-hour transitions (among ten classes of cloudiness index).

– An average temperature profile $\boldsymbol{T}_{ej}$ (°C) for each type of day j is used to model the main component of the external temperature.

– A different set of five probability matrices and four temperature profiles for each month of the heating season have been identified to characterize the evolution of solar irradiance and the external temperature.

The building model is a linear equation describing the thermal evolution of the building system:

$$\boldsymbol{T}(t+\Delta t) = g(\boldsymbol{T}(t), \boldsymbol{y}(t), \boldsymbol{u}(t)) = \mathbf{A}\boldsymbol{T}(t) + \mathbf{B}\boldsymbol{y}(t) + \mathbf{D}\boldsymbol{u}(t) \quad (2)$$

where the thermal state of the building system $\boldsymbol{T}(t+\Delta t)$ (temperatures of three building elements) depends on the previous thermal state $\boldsymbol{T}(t)$, the driving variables $\boldsymbol{y}(t)$ (solar irradiance, external and adjacent room temperatures) and the command $\boldsymbol{u}(t)$ (heating energy).

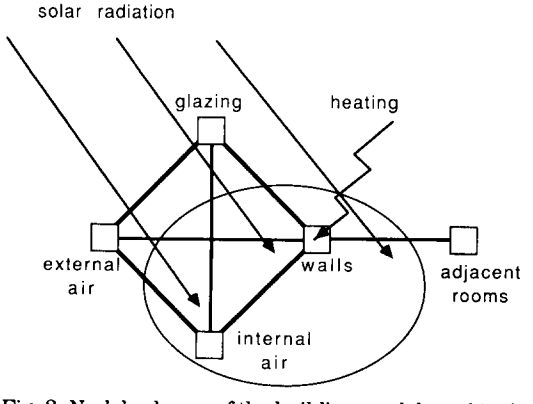

Fig. 2. Nodal schema of the building model used in the predictive controller.

The matrices **A**, **B** and **D** depend on the thermal capacity and the heat transfer between the elements of the building system. Their derivation is given in the Appendix. The different nodes and their interactions are given in Fig. 2.

The objective of the *control algorithm* is to minimize the expected cost function over the optimization period $0 \rightarrow N$:

$$\min_{\boldsymbol{u}_0, \boldsymbol{u}_1, \ldots, \boldsymbol{u}_{N-1}} E_{\boldsymbol{y}_0, \boldsymbol{y}_1, \ldots, \boldsymbol{y}_{N-1}} \left[J(\boldsymbol{u}_0, \boldsymbol{u}_1, \ldots, \boldsymbol{u}_{N-1}, \boldsymbol{T}_1, \boldsymbol{T}_2, \ldots, \boldsymbol{T}_N) \right] \quad (3)$$

where

$$J(\boldsymbol{u}_0, \boldsymbol{u}_1, \ldots, \boldsymbol{u}_{N-1}, \boldsymbol{T}_1, \boldsymbol{T}_2, \ldots, \boldsymbol{T}_N) = \sum_{k=0}^{N-1} C_1 \cdot J_1(\boldsymbol{u}_k) + C_2 \cdot J_2(\boldsymbol{T}_{k+1}) \quad (4)$$

J_1 and J_2 are defined as in eqn. (1). Equation (3) is optimized with the constraints of the evolution of the thermal state of the building system.

The expected cost is minimized according to the expected solar irradiance given by the meteorological model.

The intermediate cost f_k which is the minimum expected cost function from period k until the end of the optimization period is calculated, using dynamic programming techniques [7], for each time step k where $f_N = 0$ and k: $N-1 \rightarrow 0$. f_0 is the minimum expected cost function over the optimization period $0 \rightarrow N$ as defined in eqn. (3). The intermediate cost function is given by:

$$f_k(\boldsymbol{T}_{k-1}, \boldsymbol{y}_{k-1} = i, \boldsymbol{u}_{k-1}) = \min_{\boldsymbol{u}_k, \ldots, \boldsymbol{u}_{N-1}} EJ(\boldsymbol{u}_k, \ldots, \boldsymbol{u}_{N-1}, \boldsymbol{T}_{k+1}, \ldots, \boldsymbol{T}_N) \quad (5)$$

and calculated using:

$$f_k(\boldsymbol{T}_{k-1}, \boldsymbol{y}_{k-1} = i, \boldsymbol{u}_{k-1}) = \min_{\boldsymbol{u}_k} \sum_{j=1}^{10} P_{ij} \cdot (J(\boldsymbol{u}_k, \boldsymbol{T}_{k+1}) + f_{k+1}(\boldsymbol{T}_k, \boldsymbol{y}_k = j, \boldsymbol{u}_k)) \quad (6)$$

where P_{ij} represents the probability to change from the cloudiness index i (solar irradiance $\boldsymbol{y}_{k-1} = i$) during period $k-1$ to cloudiness index j (solar irradiance $\boldsymbol{y}_k = j$) during period k given the type of day the previous day.

The optimal command u_k^* is obtained as a function of the state of the variables:

$$u_k^* = u_k^*(\boldsymbol{T}_{k-1}, \boldsymbol{y}_{k-1}, \boldsymbol{u}_{k-1}) \tag{7}$$

The optimization is done from the end of the horizon to the beginning. A numerical example of the application of this procedure to calculate the control matrix is given in Fig. 3. A simplified notation has been introduced in which the value attributed to each variable corresponds to the state of the variable.

Step #1: The state $\boldsymbol{T}_k = 22$ is obtained from the previous state of temperatures $\boldsymbol{T}_{k-1} = 10$, the solar radiation $\boldsymbol{y}_{k-1} = 4$ and the previous command $\boldsymbol{u}_{k-1} = 2$.

Step #2: The resulting temperature $\boldsymbol{T}_{k+1} = 12$ is calculated, given $\boldsymbol{T}_k = 22$ for $\boldsymbol{u}_k = 1$ and $\boldsymbol{y}_k = 1$.

Step #3: The intermediate cost $f_{k+1}(\boldsymbol{T}_k = 22, \boldsymbol{y}_k = 1, \boldsymbol{u}_k = 1)$ is retrieved from memory, added to the cost $J(\boldsymbol{u}_k = 1, \boldsymbol{T}_{k+1} = 12)$ and multiplied by the probability P_{41}.

Step #4: Steps #2 and #3 are repeated for the other ten possible states of solar radiations and the results in #3 are summed:

$$\sum_{j=1}^{10} P_{4j}[J(\boldsymbol{u}_k = 1, \boldsymbol{T}_{k+1} = g(\boldsymbol{T}_k = 22, \boldsymbol{y}_k = j, \boldsymbol{u}_k = 1)) + f_{k+1}(\boldsymbol{T}_k = 22, \boldsymbol{y}_k = j, \boldsymbol{u}_k = 1)] = 3759$$

Step #5: The calculation of the cost, steps #2 to #4, are repeated for the other possible commands:

$$\sum_{j=1}^{10} P_{4j}[J(\boldsymbol{u}_k = 2, \boldsymbol{T}_{k+1}) + f_{k+1}(\boldsymbol{T}_k, \boldsymbol{y}_k = j, \boldsymbol{u}_k = 2)] = 2785$$

$$\sum_{j=1}^{10} P_{4j}[J(\boldsymbol{u}_k = 3, \boldsymbol{T}_{k+1}) + f_{k+1}(\boldsymbol{T}_k, \boldsymbol{y}_k = j, \boldsymbol{u}_k = 3)] = 2093$$

$$\sum_{j=1}^{10} P_{4j}[J(\boldsymbol{u}_k = 4, \boldsymbol{T}_{k+1}) + f_{k+1}(\boldsymbol{T}_k, \boldsymbol{y}_k = j, \boldsymbol{u}_k = 4)] = 2931$$

$$\sum_{j=1}^{10} P_{4j}[J(\boldsymbol{u}_k = 5, \boldsymbol{T}_{k+1}) + f_{k+1}(\boldsymbol{T}_k, \boldsymbol{y}_k = j, \boldsymbol{u}_k = 5)] = 3921.$$

Step #6: The minimum value of the sum obtained in step #5 which is the value of $f_k(\boldsymbol{T}_{k-1} = 10, \boldsymbol{y}_{k-1} = 4, \boldsymbol{u}_{k-1} = 2)$, and the corresponding optimum command, $\boldsymbol{u}_k^* = 3$, are stored in memory.

Step #7: The steps #1 to #6 are repeated for all states of $\boldsymbol{T}_{k-1}$, $\boldsymbol{y}_{k-1}$ and $\boldsymbol{u}_{k-1}$.

Step #8: The steps #1 to #7 are repeated for the previous time step, until the beginning of the optimization period.

The optimum command for each state is stored in the matrix of optimal commands. It is retrieved every hour using the measured present state of the

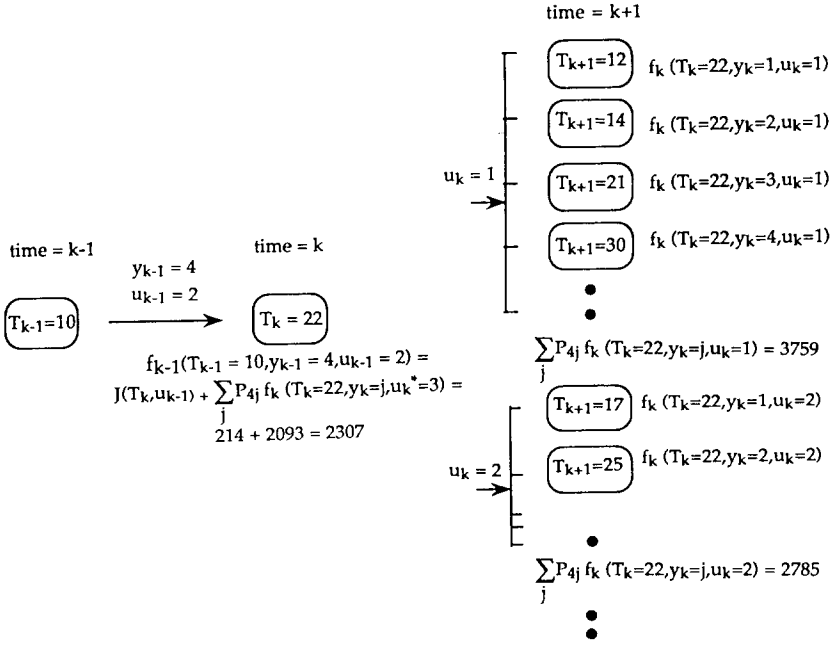

Fig. 3. Example of the calculation of the control matrix. The value attributed to the variable corresponds to the state of the variable.

building system, the state of the driving variables and the command, as pointer.

Experimental evaluation

The performance of the predictive controller was investigated in a full-scale experiment and compared with the simulation results.

A prototype of the predictive controller based on the optimal stochastic control theory was developed and implemented in an office of the LESO (Laboratoire d'énergie solaire) experimental building [14] during the winter of 1989/90. This building is situated in Lausanne (lat. 46.5 °N, alt. 410 m), by Lake Geneva in a continental climate. It is necessary to use heating during approximately 200 days of the year ($T_e > 12$ °C) in this location. The average external temperature during these days is 3.9 °C and the total solar radiation on a horizontal surface is 1453 MJ/m^2. The design temperature is −6 °C [15]. The experiment was carried out from November 15, 1989, until March 19, 1990, which included the entire heating period of the winter 1989/90.

The performance of the predictive controller was compared to that of a conventional external temperature controller in an identical office. The controllers were interchanged every two weeks in order to avoid any bias due to differences in the occupants' behaviour or in the offices. The free gains, i.e., heat dissipated by occupants and artificial lighting, were monitored as well as the difference in thermal state between the offices at the time of change-over. Both of these parameters indicate that the change-over was sufficient to eliminate any bias.

Building system

The building system used for the experimental evaluation of the predictive controller is one solar unit of the LESO experimental building. The unit was separated into two offices which are mirror images of each other. A photograph of the interior of one of these offices is given in Fig. 4.

The volume of each office is 39 m^3 and the thermal conductance from the internal to the external air is $P = 19$ W/K. The air renewal rate through infiltration has been measured and is $n \leqslant 0.1$ h^{-1}. The supplementary fresh air is supplied through window and door openings.

Double-glazed windows with IR film cover 4.0 m^2 of the south-facing wall in each office. The energy transmittance of the glazing is $G = 0.62$ and the thermal conductivity is $U = 1.3$ W/m^{2}K.

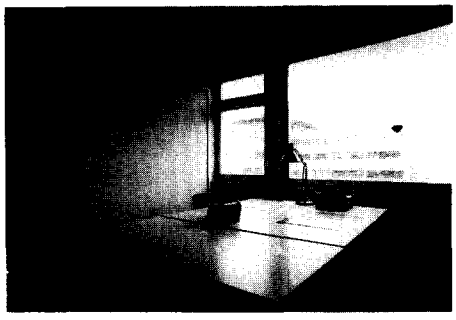

Fig. 4. Photograph of the interior of one office used in the experiment.

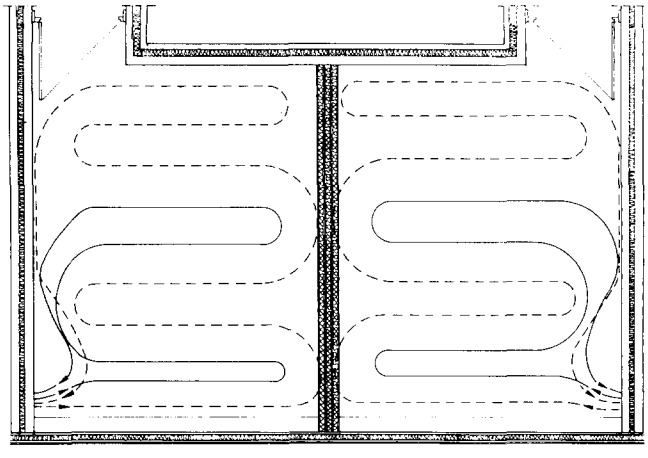

Fig. 5. The location of the heating tubes in the two offices used in the experiment.

Heating system

A floor heating system using water as a medium was installed in the building at the time of construction. The heating tubes were placed between the insulation and the mortar.

The thermal conductivity from the tubes to the surface of the floor was estimated at 23 W/m^{2}K whilst the conductivity from the tubes to the surface of the ceiling below was estimated at 0.53 W/m^{2}K. This implies that only 2% of the heating energy is lost to the room below if the air temperatures of the two offices are the same. A thermo-camera was used to identify the location of the tubes in the floor. Figure 5 indicates the location of the tubes, as well as the thermal insulation.

The water pipes were equipped with two immersion heaters of 400 W and 800 W in each office, and an electric pump which dissipates 30 W in the east office and 40 W in the west office. The power supplied to each office can therefore be either 0 W, 400 W, 800 W or 1200 W during any time period, in addition to the power from the pump. The controls of the heating systems are located outside the two offices and they can be easily interchanged.

Prototype predictive controller

The prototype predictive controller was implemented on an IBM-compatible personal computer using the DOS operating system and the programming language QuickBasic. An Analog Connection ® board and a mathematical co-processor were installed for the data acquisition and control. The calculation of the control matrix takes approximately two hours on this machine, although most of the calculation time is used to store and retrieve data from disk.

Three temperature measurements were made in each room, an ambient internal air temperature, a "comfort" temperature (average of air and radiant temperatures), and a floor temperature at a depth of 2 cm. The global horizontal solar irradiance and the external temperature were also measured. The temperatures were measured using Pt-100 sensors and the solar irradiance using an Eppley Pyranometer PSP.

Conventional controller

The conventional control system that was used in the experiment is a commercially available product TEM Polymat. It is an external temperature controller, consisting of an external temperature sensor, a water temperature sensor situated just after the immersion heaters, and a control box. The heating curve is identified by seven parameters that are present on the control box. These are the gradient and the off-set of the heating-curve, the cut-off temperature, the night set-back, the heating type (normal, set-back, no freezing, off), a timer and security.

Two weeks of measurements in cloudy conditions, when the external temperature varied between −3 °C and +12 °C were used to estimate the heating needs of the system in the steady state. The relation found between the internal temperature θ_i, the water temperature θ_w, and the external temperature θ_e was:

$$\langle\theta_i\rangle = 3.66\ °C + 0.633\langle\theta_w\rangle + 0.215\langle\theta_e\rangle \quad (8)$$

As indicated in eqn. (8) the free and solar gains contribute 3.66 °C of the internal air temperature. By setting the internal temperature equal to the desired internal temperature, $\theta_i = 20$ °C during the day, it was possible to calculate the desired heating curve:

$$\theta_w(\theta_e) = 25.8\ °C - 0.34\theta_e \quad (9)$$

Data acquisition system

A data acquisition system was installed in the LESO experimental building at the time of construction, 1982. Several different kinds of sensors were installed in order to determine the thermal state of each solar unit and of the building in general. There are 44 sensors installed in the test unit consisting of the two offices used in this experiment and 22 sensors are used to determine the meteorological conditions of the building. The value of each of the sensors is read by the data acquisition system every minute. The average or the integral of these values is stored on magnetic tape every half hour.

Results

The analysis of the results concentrates on energy consumption and the thermal comfort of the occupants.

Energy consumption

The energy consumed by the two control systems was compared. The heating energy consumption for the entire heating season was 27% less with the predictive controller, as indicated in Fig. 6. The solar, free, and heating gains have been measured, the heat losses estimated using the thermal loss coefficient and the internal-external temperature difference. The utilized and rejected gains have been deduced from these values and they are accurate to within 10%.

The superior energy performance of the predictive controller is also illustrated by the difference in the rejected solar gains, which were 45% for the conventional controller and 29% for the predictive controller.

A more detailed comparison shows the difference in strategy between the two controllers. The principle of the predictive controller is to utilize the solar gains for heating to a larger extent than the conventional controllers.

Week-by-week comparisons of solar and heating gains and the external temperature, as given in Fig. 7, show that the difference in efficiency between the predictive controller and the conventional controller increased with the solar gains. There was no difference in the energy consumption of the two controllers for periods with small solar gains, i.e., less than 200 W as average on a week ($\langle E_{vs}\rangle \leqslant 50$ W/m^2). An exception is week 52, when the conventional controller consumed less energy than the predictive controller. The solar and free gains did not correspond to the implemented heating curve and thermal comfort was poor in the office with the conventional controller. The energy savings for the predictive controller were as high as 35% for

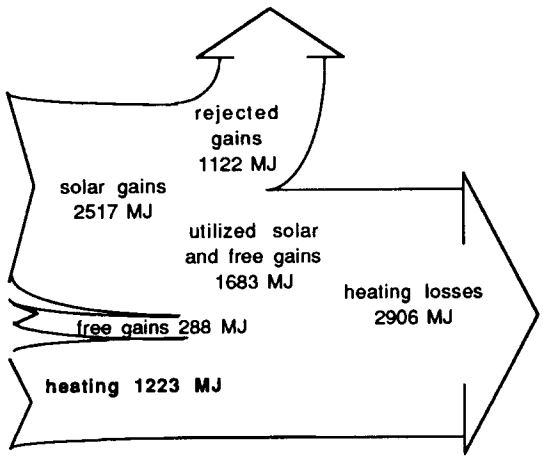

(a)

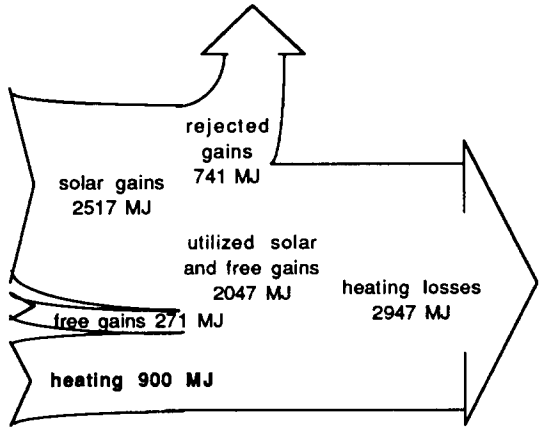

(b)

Fig. 6. Thermal flux through the building system with (a) the conventional controller and (b) the predictive controller; heating season 1989–90.

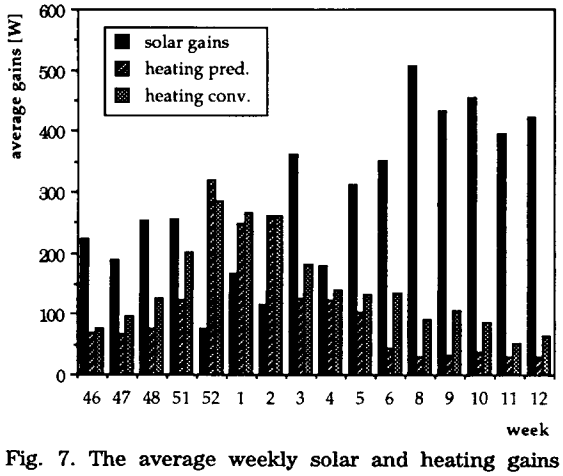

Fig. 7. The average weekly solar and heating gains for the investigated systems. Data from "weekly data experiment".

one week during the colder period of the winter. During the warmer heating period the savings varied between 10% for a week with only one sunny day, to 65% for a cool and sunny week.

The evolution of the different gains and the ambient temperatures during two typical days are given in Fig. 8. During the first day, i.e., Tuesday January 23, 1990, the solar gains are more than sufficient to heat the two offices. The predictive controller will only give small impulses to heat in the morning whilst the conventional controller will continue supplying heat until overheating occurs. During the second day, i.e., Wednesday January 24, 1990, the solar gains are far from sufficient, and the energy supplied by the two controllers is almost identical.

Thermal comfort

The thermal comfort of the occupants in the two offices has been estimated in two different ways based on Fanger's theory [13] of votes of thermal comfort.

The first evaluation is based on temperature measurements in the two offices 24 hours a day, seven days a week, irrespective of whether they were occupied. The result is given in Fig. 9(a). The high frequency of overheating is mainly explained by the calculation of PMV even when there were no oc-

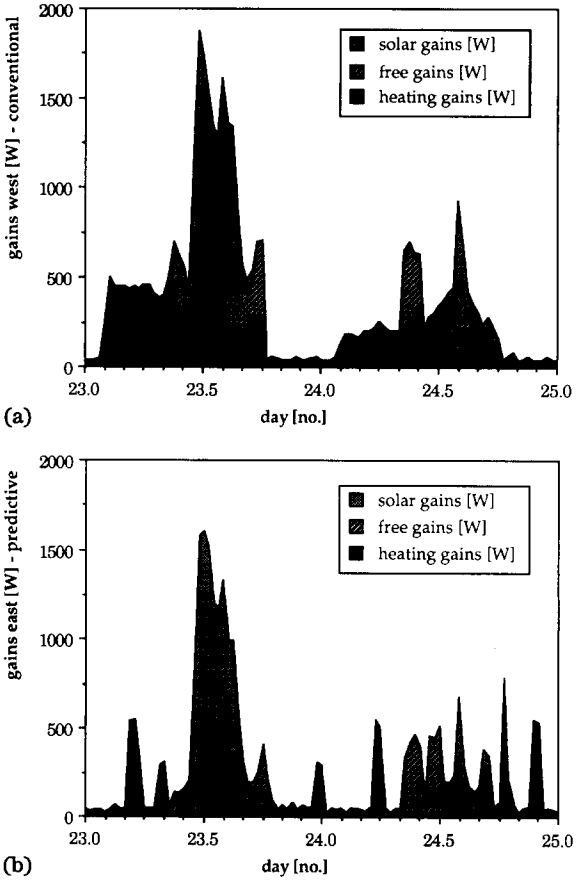

Fig. 8. The evolution of the different gains for two typical days in the office with (a) the conventional controller, and (b) the predictive controller. Data from "dalle367.cri;2".

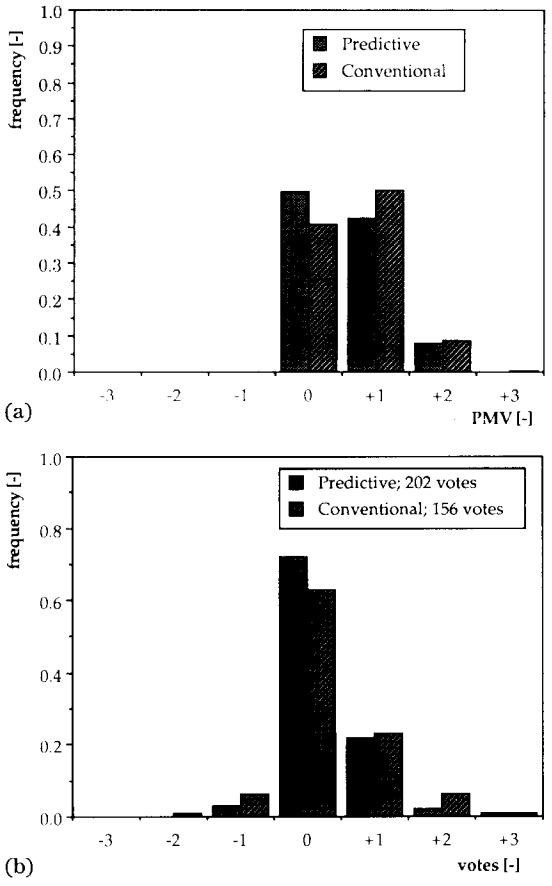

Fig. 9. PMV in the two offices: (a) obtained by temperature measurements and (b) the votes of thermal comfort given by the occupants in the same offices. Data from "vote 103–104".

cupants who could reject the excess heat by window openings. The histograms show, however, that the thermal comfort in the office with the predictive controller is better.

This is confirmed by the survey of actual occupants' votes as given in Fig. 9(b). The occupants were asked to note their thermal comfort in the mornings and in the afternoons. The votes give an accurate picture of the actual perceived comfort and they are by definition only given during occupancy periods. However, there is still overheating, mainly because the external blinds had been set in an open position to ensure the same solar gains in both offices. There are two possible disadvantages with this method. Firstly the occupants might be biased if they know the configuration of controllers and offices. Secondly they may forget to note their votes at times and data is lost.

The analysis shows that the thermal comfort in the office with the predictive controller is improved compared to that with the conventional controller. Temperatures below the comfort level were only experienced once and this was in the office with the conventional controller during week 52. The temperature in the east office was consequently lower than in the west office by ~0.5 °C on average and 1–2 °C during occupied periods.

Conclusions

The objective of this study was to investigate the possibility of improving thermal control of building systems by developing a controller that accounts for the random nature of the driving variables, in this case solar radiation and external temperature. This controller should maintain or improve the thermal comfort of the occupants while reducing the primary energy consumption of the building system.

The solar gains and the external temperature have been identified as the two most important driving variables of the investigated building systems. The random nature of the global solar irradiance on a horizontal surface was accounted for by the development of stochastic models based on Markov chains. Daily profiles were identified to account for the future temperature evolution.

A prototype of the predictive controller based on the optimal stochastic control theory was developed and implemented in an office of the LESO experimental building during the winter of 1989/90. The performance of this controller was compared to that of a conventional external temperature controller in an identical office. The controllers were interchanged every two weeks in order to avoid any bias due to differences in the offices or the occupants. The experiment showed that this controller can operate in realistic conditions and the results obtained correspond to the computer simulations.

The experimental comparison between the two offices has shown that the energy consumption was 27% lower in the office with the predictive controller than in the office with the conventional controller. Typical examples of energy consumption were as follows:

- The energy consumption in the two offices was identical for cloudy winter weeks.
- The predictive controller consumed 35% less energy than the conventional controller for a very sunny week in the middle of the winter.
- For weeks during the warmer period the measured reduction in energy consumption varied between 10% and 60%.

Other significant observations concerning the thermal comfort were that:

- The thermal comfort of the occupants was improved in the office with the predictive controller.

• Overheating occurred in both offices but energy equal to 29% of the solar gains was rejected in the office with the predictive controller and 45% in the office with the conventional controller.

This type of controller is especially suited for passive solar systems combined with large inertia heating systems.

An important development effort would be necessary to obtain a commercially available predictive controller based on optimal stochastic control. This would typically be an electronic card containing the control algorithm which could be implemented in generally available heating systems at reasonable cost.

Improvements in the performance of the controller could be obtained by using models of free gains in buildings where these gains account for a significant part of the heating required.

The generalization of the controller to other building systems might imply an increase in the number of necessary states. The first step of such a generalization would be the simulation and the measurement of other building systems.

A logical extension would be to use this controller not only for the control of heating plants but also for cooling plants and combined heating and cooling plants.

The application of this type of controller to other areas where the solar irradiance has a large influence on the performance can also be envisaged, e.g., active solar and photovoltaic cells.

Nomenclature

$\boldsymbol{T}$	vector of temperatures, state variables (K)
$\boldsymbol{y}$	vector of driving variables
$\boldsymbol{u}$	vector of commands
$g()$	linear model of building evolution $\boldsymbol{T}(t+\Delta t)=g(\boldsymbol{T}(t),\ \boldsymbol{y}(t),\ \boldsymbol{u}(t))=\mathbf{A}\boldsymbol{T}(t)+\mathbf{B}\boldsymbol{y}(t)+\mathbf{D}\boldsymbol{u}(t)$
t	time (s)
Δt	time step (s)
A, **B**, **D**	matrices
J	cost function
C_1, C_2	weight of energy consumption and thermal comfort terms respectively, in the cost function
PMV	predicted mean vote
E	solar irradiance (W/m^2)
E_h	solar irradiance on a horizontal surface (W/m^2)
E_h0	potential solar irradiance on a horizontal surface (W/m^2)
τ	cloudiness index
$\langle E_\mathrm{h}\rangle_j$	average solar irradiance on a horizontal surface for the day j (W/m^2)
$\langle E_\mathrm{h0}\rangle_j$	average potential solar irradiance on a horizontal surface for the day j (W/m^2)
r	fraction of average daily irradiance
$\boldsymbol{T}_k$	vector of temperatures, state variables, at time step k (K)
$\boldsymbol{y}_\mathrm{k}$	vector of driving variables at time step k
$\boldsymbol{u}_k$	vector of commands at time step k
$u_k{}^*$	optimal command at time step k
f_{k-1}	intermediate cost function from time step $k-1$ until the end of the optimization period
P_{ij}	transition probability from state i to state j
n	ventilation rate (h^{-1})
P	specific loss of building system (W/K)
G	energy transmittance
U	thermal transmittance (W/m^{2}K)

References

1 T. Hartman, Dynamic control of heat called key to saving energy, *Air Condit., Heat. Refrig. News*, Sept 1, 1980.

2 M. M. Shapiro, A. J. Yager and T. H. Ngan, Test hut validations of a microcomputer predictive HVAC control, *ASHRAE Trans., 94* (Part 1) (1988) 644–663.

3 T. Itoh, A. Shimizu and A. Takahashi, An advisory system for comfort control operation of HVAC systems in multistorey buildings, *Proc. CLIMA 2000, Sarajevo, Yugoslavia, Aug. 24–Sept. 1, 1989.*

4 R. C. Winn and C. B. Winn, Optimal control of auxiliary heating of passive-solar-heated buildings, *Solar Energy, 35* (1985) 419–427.

5 P. Parent and P. Morand, Application of optimal control theory to building energy management systems, *Proc. ICBEM '87, Lausanne, Switzerland, Sept. 28–Oct. 2, 1987.*

6 A. H. C. van Paassen, Passive solar energy in the intelligent buildings. *ASHRAE Trans., 94* (Part 1) (1988).

7 P. P. Bertzekas, *Dynamic Programming and Stochastic Control*, Academic Press, New York, 1976.

8 M. Nygård Ferguson and J.-L. Scartezzini, Computer simulations of an optimal stochastic controller applied to passive solar rooms, *Energy Build., 14* (1989) 1–7.

9 M. Nygård Ferguson, Predictive thermal control of building systems, *Ph.D. Thesis*, EPFL, Lausanne, 1990.

10 J. Tödtli, Optimierungsideen für den betrieb von HLVC anlagen, *SGA Zertschift, 5* (1985).

11 D. Heinemann and J. Luther, Control of renewable energy systems using Bayesian forecasting techniques and stochastic dynamic programming, *Proc. ISES Solar World Congress, Kobe, Sept. 1989*, Pergamon, 1990.

12 K. J. Åström, Theory and application of adaptive control – A survey, *Automatica, 19* (1983) 471–486.

13 P. O. Fanger, *Thermal Comfort*, R. E. Krieger, Malabar, FL, 1982.

14 J.-L. Scartezzini, A. Faist and J.-B. Gay, Experimental comparison of a sunspace and a water hybrid solar device using the LESO test facility, *Solar Energy, 38* (1987) 355–366.

15 A. Faist *et al.*, *Guide Solaire Passif*, Ecole Polytechnique Fédérale de Lausanne, Switzerland, 1985.

Appendix

A building model of the form:

$$T_i(t+\Delta t)=\sum_j[\mathbf{A}_{ij}\boldsymbol{T}_j(t)+\mathbf{B}_{ij}\boldsymbol{y}_j(t)+\mathbf{D}_{ij}\boldsymbol{u}_j(t)]$$

has been determined where:

$$\mathbf{A}_{ij}=S_{ij}{}^{-1}\mathrm{C}_j$$

$$\mathbf{B}_{i1}=\sum_{k=1}^{N_f}S_{ik}{}^{-1}\cdot\Delta t\cdot S$$

$$\mathbf{B}_{i2}=\sum_{k=1}^{N_f}S_{ik}{}^{-1}\cdot\Delta t\cdot H_{\mathrm{e}\to k}$$

$$\mathbf{B}_{i3}=\sum_{k=1}^{N_f}S_{ik}{}^{-1}\cdot\Delta t\cdot H_{\mathrm{adj}\to k}$$

$$\mathbf{D}_{ik_0}=S_{ik}{}^{-1}\cdot\Delta t$$

$$\boldsymbol{S}_{ii}=C_k+\sum_{\substack{j=1\\ j\neq i}}^{N}H_{j\to i}\cdot\Delta t$$

$$S_{ik}=-H_{k\to i}\cdot\Delta t\quad(\forall k\neq i)$$

where N=number of nodes, N_f=number of nodes which are not assigned, T_j=temperature of node j (K), C_j=heat capacity of element j (J/K), $H_{j\to i}$=thermal conductivity from element j to i (W/K), k_0=the node to which the heating energy is applied, S=the solar irradiance capture area.